

Aerosol Delivery by Inhalation Catheter and Trachea Digitalization

I. Aramendia^{1*}, U. Fernandez-Gamiz¹, A. Lopez-Arraiza², M.A. Gomez-Solaetxe², L. Barrenetxea³, E. Solaberrieta³, R. Minguez³, J. Sancho¹

¹ Nuclear Engineering and Fluid Mechanics Department, University of the Basque Country UPV/EHU, Vitoria-Gasteiz, Araba, Spain,

² Department of Nautical Science and Marine Systems, University of the Basque Country UPV/EHU, Portugalete, Bizkaia, Spain.

³ Department of Graphic Design and Engineering Projects, University of the Basque Country UPV/EHU, Bilbao, Bizkaia, Spain.

*corresponding author: inigo.aramendia@ehu.eus

Abstract

Neonatal respiratory distress syndrome (RDS) is related with high mortality and morbidity in preterm infants and the best approach to treat it is an open research field. The use of perfluorocarbons (PFC) together with non-invasive respiratory support techniques, such as nasal continuous positive airway pressure (CPAP), has confirmed its effectiveness to achieve a more homogeneous surfactant distribution. The goal of the current study was to evaluate the main features of the aerosol generated by an intracorporeal inhalation catheter, which consists of one central lumen delivering the liquid and six peripheral lumens delivering compressed air. Firstly, experiments were made through an Aerodynamic Particle Sizer (APS) with sterile water and perfluorocarbon FC75 with a driving pressure of 4 bar to analyze properties linked with lung deposition such as the aerodynamic diameter (D_a), mass median aerodynamic diameter (MMAD) and geometric standard deviation (GSD). Subsequently, a numerical model was developed with CFD techniques. The experimental validation of the numerical model provides an accurate prediction of the air flow axial velocity.

1. Introduction

Extremely and very preterm infants present cerebral and pulmonary issues due to the immaturity of the lungs, primarily caused by the lack of surfactant. This leads to the Respiratory Distress Syndrome (RDS) of the newborn, which is the leading cause of death in premature babies [1]. This natural substance covers the alveoli, its main goal being to reduce the surface tension and, therefore, to prevent alveolar collapse at the end of the exhalation, retaining enough air to start the next breath.

The current surfactant replacement therapy implies some drawbacks, as the requirement of intubation and the application of ventilator support techniques, which can result in lung injury and chronic lung diseases (CLD) [2]. In this regard, the neonatologists are focused on new minimally invasive surfactant therapies (MIST) as an alternative to solve the current dilemma; how to deliver exogenous surfactant without invasive techniques when the application of continuous positive airway pressure (CPAP) is not enough [3].

The administration of nebulized surfactant is a promising technique to treat lung diseases and especially RDS, even though there are still technical issues and challenges to lead. Four clinical trials have been published showing that is a feasible and safe technique. However, only one of them [4] has demonstrated good results. Currently, Pillow and Minocchieri are working on a new clinical trial, the CureNeb study, where preterm infants receive either CPAP or CPAP and nebulized surfactant in the first 4 hours of life [5]. Another alternative is the use of perfluorocarbons (PFC). Burkhardt et al. [6] have demonstrated that is useful to improve surfactant distribution and that resulted in an improved oxygenation.

One of the main reasons of the low efficiency of nebulized surfactants in these clinical trials is the relative low lung deposition rates (less than 1% of the mass nebulized) with conventional jet and ultrasonic nebulizers. Nevertheless, Goikoetxea et al. [7] have studied the potential to deliver relatively large amounts of surfactants and perfluorocarbons beyond the third generation of branching in a neonatal airway model through an intracorporeal inhalation catheter (IC). The influence of four different ventilation strategies on surfactant and PFC aerosol production rate were studied in an *in vitro* study by Murgia et al. [8]. The results showed that higher peak inspiratory pressure (PIP) and higher respiratory rates (RR) might enhance surfactant and PFC delivery to the lungs but might also increase compound loss during expiratory phase.

Numerical models through Computational Fluid Dynamics (CFD) techniques provide a useful methodology to study the behavior of aerosol particles in the airways and to obtain valuable data related with airflow patterns, particle deposition and particle size distributions. Recently, Goikoetxea et al. [9] evaluated with a numerical model the aerosol delivery of surfactant and perfluorodecalin (PFD) by means of an inhalation catheter (IC). The results showed the beneficial effects of generating an intracorporeal aerosol with minimal airway manipulation.

2. Experimental Setup

An inhalation catheter (IC) (AeroProbe, Trudell Medical International), illustrated in Fig. 1, was used to produce the aerosol. Sterile water (H₂O_d) has been used to simulate the nebulization. The compressed air is delivered through six peripheral lumens and the liquid is delivered through the central lumen. The close proximity of these lumens at the catheter tip results in efficient aerosolization of the liquid. Additionally, the perfluorocarbon (PFC) compound FC-75 (C₈F₁₆O) has been tested.

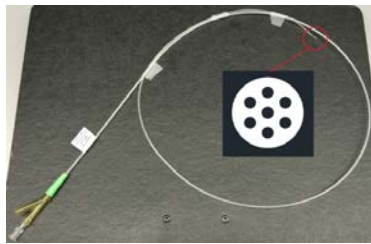


Figure 1. Inhalation catheter (IC 1.1)

An Aerodynamic Particle Sizer (APS 3321) has been used, which provides high-resolution of particles from 0.5 to 20 μm. The IC has been connected to a pressure control system, which allows to change the driving pressure between 0-7 bar. The scheme of Fig. 2 shows the equipment and experimental setup used to study the aerosol formation. The distal end of the IC has been aligned with the nozzle of the APS in order to obtain an accurate measurement of the aerosol generated and different distances between the distal end of the IC and the nozzle has been set to check the concentration of the aerosol. Even though the usable data of the APS is up to 10.000 particles/cm³, the average recommended particle concentration is 1000 particles/cm³

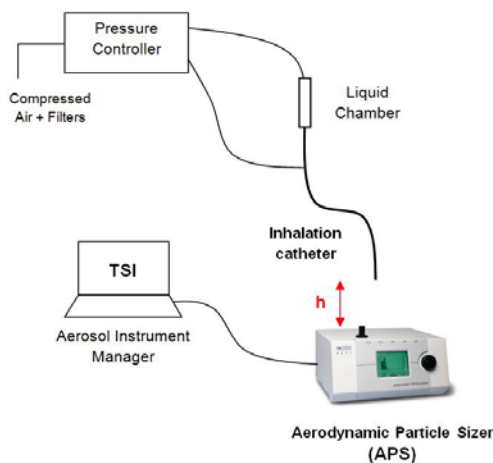


Figure 2. Experimental setup

3. Experimental results

Both compounds were studied with a driving pressure of 4 bar, as can be seen in Tables 1-2. Five samples were recorded for each case, with a sample time of 10 seconds. At first, it was necessary to establish the optimal distance between the catheter tip and the APS nozzle in order to obtain accurate measurements. It was found that the

optimal distance were 42 cm and 5.2 cm for the sterile water (H₂O_d) and the FC-75 respectively.

Sample	Da (μm)	MMAD (μm)	GSD	Concentration (particles/cm ³)
16	4.00	10.3	2.20	1040
17	4.09	10.3	2.19	1210
18	4.08	10.1	2.15	1240
19	4.12	9.89	2.14	1060
20	4.01	10.2	2.21	1050
MEAN	4.06	10.16	2.18	
SD	0.05	0.17	0.03	

Table 1. Experimental results with sterile water

The same procedure was carried out with the FC-75 compound with a driving pressure of 4 bar and its optimal distance. This data were used to validate the results of the numerical model.

Sample	Da (μm)	MMAD (μm)	GSD	Concentration (particles/cm ³)
1	2.47	10.5	1.70	1140
2	2.45	10.1	1.69	1160
3	2.44	10.3	1.70	1190
4	2.45	9.73	1.68	1210
5	2.43	9.42	1.68	1140
MEAN	2.45	10.01	1.69	
SD	0.01	0.44	0.01	

Table 2. Experimental results with FC75 compound

The geometric standard deviation (GSD), the mass median aerodynamic diameter (MMAD) and the aerodynamic diameter (Da) have been analyzed to study the particle size characterization. The GSD is a dimensionless number which gives an indication of the spread of sizes of particles that make up the aerosol. An aerosol is made up of particles of many different sizes (heterodisperse aerosol) with a GSD above 1.25. On the other hand, a GSD below 1.25 indicates that all the aerosol particles are of the same or very nearly the same size (monodisperse aerosol). The MMAD is defined as the value of the aerodynamic diameter (Da) such that half the mass of the aerosol is contained in small diameter particles and half in larger. The relationship between the aerodynamic particle diameter (Da) measured by the APS and the geometric particle diameter (Dg) is given by (1):

$$D_g = D_a \sqrt{\frac{\rho_0}{\rho}}$$

where ρ₀ is the unit density (1 g/cm³) and ρ the density of the compound to be nebulized, in this case ρ = 0.9982 g/cm³ for the sterile water and ρ = 1.78 g/cm³ for the FC75 compound.

4. Numerical model

In the work presented in this study the commercial CFD code Star CCM+ version 11.06 (CD Adapco®) was used to create and run the numerical model. The problem was simplified making an axisymmetrical assumption to define the computational domain in order to save

computational time in the simulation of the discrete particles. In this case, the six outer lumens are replaced by a ring, as shown in Fig. 4. The position of the air lumen (b_{lcn}) was maintained and the width of the ring was calculated by (3-5) in order to have the same area of the six outer lumens and consequently, the same air mass flow. The computational domain consists of the last 2 mm of the catheter and the downstream region beyond the catheter tip, as illustrated in Fig. 3. The outlet is located 52 mm away from the catheter tip, which is the optimal distance used for the experimental measurement of the FC-75 particle size distribution with the APS.

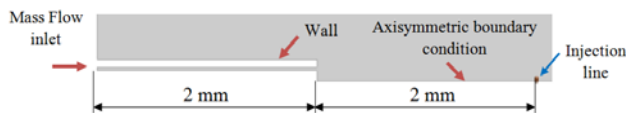


Figure 3. Computational domain and boundary conditions

An air mass flow rate of 1.1344×10^{-5} kg/s, measured in a previous work with a driving pressure of 4 bar [7], was defined as the inlet boundary condition along with a temperature of 293K and a turbulence intensity of 0.07. An atmospheric outlet boundary condition was fixed for downstream boundaries and the axisymmetrical condition was set to the central axis. Ten particle injections were defined, as can be seen in Table 3, to represent the particle size and mass distribution. The injection line was defined 2 mm away from the catheter tip as an estimated value between the APS nozzle and the laser beams which measures the distribution of the particles.

Injection	D_g (μm)	Mass flow rate (kg/s)
1	0.392	$3.41 \cdot 10^{-8}$
2	0.604	$2.68 \cdot 10^{-8}$
3	0.866	$3.17 \cdot 10^{-7}$
4	1.335	$2.41 \cdot 10^{-7}$
5	1.910	$6.88 \cdot 10^{-7}$
6	2.945	$1.20 \cdot 10^{-5}$
7	4.535	$6.31 \cdot 10^{-6}$
8	6.495	$1.55 \cdot 10^{-6}$
9	10.000	$1.61 \cdot 10^{-6}$
10	14.850	$4.90 \cdot 10^{-7}$

Table 3. Particle initial conditions obtained from experimental measurements

5. Numerical results and experimental validation

The continuity and Navier-Stokes equations are solved for the continuous phase (air) and the Newton's second law of motion is solved for the dispersed liquid droplets. Once the steady state air solution is converged the discrete phase was added by injection points defined within a line and simulated in transient state.

Fig. 4 illustrates the air flow velocity once the solution was converged. The highest value was reached close to the outlet of the catheter tip with a peak of 385 m/s. The velocity value 2 mm away from the outlet, where the injectors were defined, was 238 m/s [10].

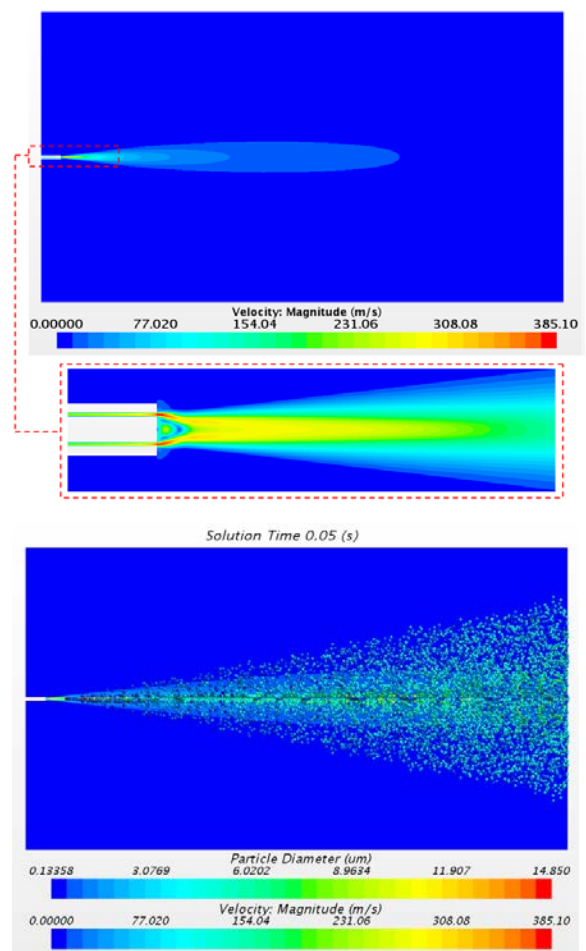


Figure 4. Continuous phase velocity magnitude and particle size distribution of the discrete particles

The axial velocity at different distances beyond the catheter tip were taken and validated with experimental data by means of a hot-wire constant temperature anemometer (Goikoetxea et al. [9]). The Realizable K-epsilon model used in the numerical model provides an accurate prediction of the air flow (See Fig.5).

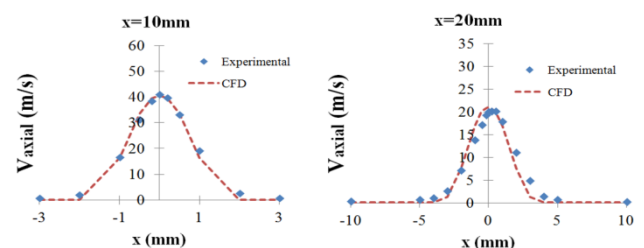


Figure 5. Experimental and numerical axial air velocity profiles

6. Trachea digitalization

A surface model was needed to perform the CFD analysis, so three tracheal segments from pigs were digitized. Initially, the pieces required to be divided in order to scan their interior. The cut would deform its inner shape due to the soft organic tissue composition of the tracheas. To minimize this situation, the exterior of the parts were previously scanned and two rigid plastic shells were prototyped from the surface. With the shells wrapping the tracheal segments, they were cut off, as

illustrated in Fig.6a. These housings fix the outer shape and minimize deformation inside the tracheal segment. The inner surface was scanned by structured blue light to filter out interfering ambient light. Afterwards, the point clouds were treated and optimized (See Fig.6b). In each case the two halves were joined together using the initial scan and shells as reference and exported to a format understandable for the CFD software (See Fig.6c). The task was carried out by the ATOS Compact Scan M5™ hardware, from GOM mbH manufacturer, and by the Geomagic Design X software, from 3D Systems Corporation.

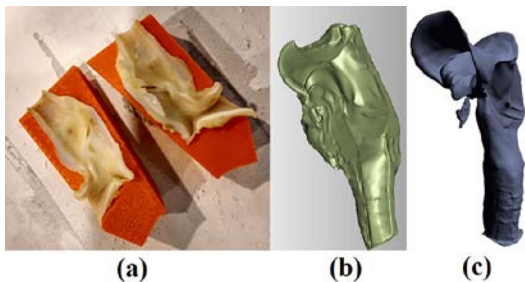


Figure 6. Process of trachea digitalization

Once the geometry was imported to the CFD code, the trachea segment was modified to add the catheter tip. An unstructured polyhedral mesh with 1.5 million cells was used in the domain, as shown in Fig. 7.

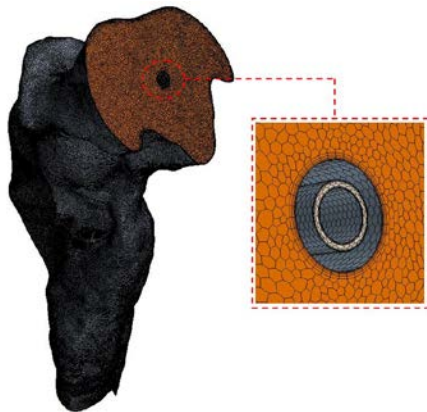


Figure 7. Mesh distribution of the geometry with the catheter tip

An air mass flow rate of $1.1344 \cdot 10^{-5}$ kg/s was defined as the inlet boundary condition to study the distribution of the velocity airflow through the trachea.

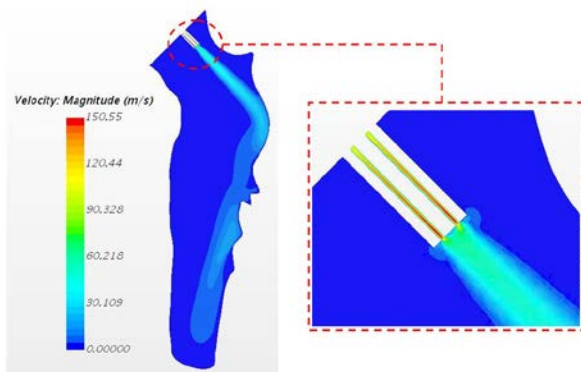


Figure 8. Numerical simulation of the air inside the trachea

7. Conclusions

The aerodynamic diameter (D_a) measured was between the optimal recommended values ($1-5 \mu\text{m}$) and even though the MMAD is around $10 \mu\text{m}$ the study is focused to generate the aerosol beyond the nasopharyngeal area, avoiding the deposition of big particles. Further work is necessary to implement the numerical model presented above to study the aerosol generated in the trachea.

Acknowledgments

This work has been supported by Consolidated Groups from the Basque Government. Technical and human support provided by IZO-SGI, SGIker is gratefully acknowledged.

References

- [1] Kamath BD, MacGuire ER, McClure EM, Goldenberg RL, Jobe AH. Neonatal mortality from respiratory distress syndrome: Lessons for low-resource countries. *Pediatrics*, vol 127, no 6, 2011, pp 1139-1146.
- [2] Jobe AH, Ikegami M. Mechanisms initiating lung injury in the preterm. *Early Human Development*, vol 53, no 1, 1998, pp 81-94.
- [3] Herting E. Less invasive surfactant administration (LISA) - Ways to deliver surfactant in spontaneously breathing infants. *Early Human Development*, vol 89, no 11, 2013, pp 875-880.
- [4] Jorch G, Hartl H, Roth B, Kribs A, Gortner L, Schaible T et al. Surfactant aerosol treatment of respiratory distress syndrome in spontaneously breathing premature infants. *Pediatric Pulmonology*, vol 24, no 3, 1997, pp 222-224.
- [5] Pillow JJ, Minocchieri S. Innovation in surfactant therapy II: Surfactant administration by aerosolization. *Neonatology*, vol 101, no 4, 2012, pp 337-344.
- [6] Burkhardt W, Kraft S, Ochs M, Proquitte H, Mense L, Rudiger M. Persurf, a new method to improve surfactant delivery: A study in surfactant depleted rats. *PLoS One*, vol 7, no 10, 2012, pp e47923.
- [7] Goikoetxea E, Murgia X, Serna-Grande P, Valls-i-Soler A, Rey-Santano C, Rivas A et al. In vitro surfactant and perfluorocarbon aerosol deposition in a neonatal physical model of the upper conducting airways. *PLoS One*, vol 9, no 9, 2014, pp e106835.
- [8] Murgia X, Gastiasoro E, Mielgo V, Alvarez-Diaz F, Lafuente H, Valls-i-Soler A et al. Surfactant and perfluorocarbon aerosolization by means of inhalation catheters for the treatment of respiratory distress syndrome: an in vitro study. *Journal of Aerosol Medicine and Pulmonary Drug Delivery*, vol 24, no 2, 2011, pp 81-87.
- [9] Goikoetxea E, Rivas A, Murgia X, Anton R. Mathematical modeling and numerical simulation of surfactant delivery within a physical model of the neonatal trachea for different aerosol characteristics. *Aerosol Science and Technology*, vol 51, no 2, 2017, pp 168-177.
- [10] Aramendia I, Fernandez-Gamiz U, Lopez-Arraiza A, Gomez-Solaetxe M.A, Lopez-Guede J.M, Sancho J, Basterretxea F.J. Computational characterization of aerosol delivery for preterm infants. *International Journal of Biology and Biomedical Engineering*, vol 11, 2017, pp 29-38